Available online at www.sciencedirect.com
ScienceDirect

Journal of Magnesium and Alloys 1 (2013) 134−138
www.elsevier.com/journals/journal-of-magnesium-and-alloys/2213-9567

Full length article

Relationship between extrusion, Y and corrosion behavior of Mg−Y alloy in NaCl aqueous solution

Kui Zhang*, Xin Zhang, Xia Deng, Xinggang Li, Minglong Ma

State Key Lab for Fabrication & Processing of Non-ferrous Metals, Beijing General Research Institute for Non-ferrous Metals, Beijing 100088, China

Abstract

The effect of hot extrusion and addition of Y element on the corrosion behavior of Mg−Y alloy was investigated by weight loss, immersion tests and potentiodynamic polarization measurements. The results showed that the grains became finer and uniform by increasing Y element, after extrusion. The corrosion resistance of Mg−Y alloy after extrusion was deteriorated with the addition of Y element and corrosion rates decreased in the following order: Mg−13.78Y > Mg−7.46Y > Mg−5.23Y.

The corrosion rate of the transversal facet was firstly nobler and then became worse than that of longitude section by increasing immersion time. The corrosion rate increased by extending immersion time, and then the corrosion rate tended to be smooth in the last stage.

Keywords: Mg−Y; Microstructure; Corrosion; Extrusion

1. Introduction

Mg−RE alloy is regarded as the most potential Mg alloy system for military products because of its excellent high temperature performance. Y is a kind of very important alloy for the Mg alloys because the standard electrode potential for both Y and Mg are −2.732 V. Therefore, Y is a preferred alloy element for Mg alloys, furthermore solid solubility of Y in Mg is 12.5%. Considerable works have reported the corrosion performance of Mg alloy containing Y such as WE54, WE43 and EW75 [1−3]. Corrosion of Mg alloy containing Y is hindered by the formation of second phase Mg24Y5 and the protective magnesium hydride on the surface. Recently, the corrosion behavior of extruded Mg alloy becomes a hot topic in the corrosion field [4,5]. Eliezer et al. [6] reported that the corrosion resistance of AZ31 alloy decreases after extrusion. Abuleil et al. [7] also reported that the extrusion process increases the corrosion resistance of Mg−Sn alloy. However, the effect of extrusion and addition of Y on the corrosion behavior of Mg−Y alloy is not properly understood until now. Therefore, this work mainly focus on the effect of extrusion and addition of Y on corrosion behavior of Mg−Y alloy in 3.5 wt.% NaCl solution.

2. Experimental methods

The compositions of as extruded alloys were Mg−5.23Y, Mg−7.46Y, and Mg−13.78Y. Extrusion was performed on a horizontal extrusion press after solution treatment at 545 °C for 24 h, while the temperature of extruding tube was 480 °C. Extrusion ratio and extrusion speed were 5:1 and 380 mm/min, respectively. The samples were directly cooled by water, during the extrusion process.

* Corresponding author. Tel.: +86 13501271756.
E-mail address: zhkui@grinm.com (K. Zhang).
Peer review under responsibility of National Engineering Research Center for Magnesium Alloys of China, Chongqing University

Production and hosting by Elsevier

http://dx.doi.org/10.1016/j.jma.2013.07.002

The samples were prepared with dimensions of 10 mm × 10 mm × 10 mm and encapsulated in cold setting resin. The microstructures were investigated using the Carl Zeiss Axiocert 2000MAT. 5 ml HNO_3 in 95 ml ethanol was used as etching reagent. A potentiostat/Galvanostat Model 273A was used for the electrochemical measurements. The polarization measurements were carried out at a scan rate of 0.5 mV/s, from −100 mV to +400 mV with respect to the corrosion potential (E_{corr}).

The evolved hydrogen gas was collected in a burette above the samples. The samples were immersed in solution of 200 g CrO_3 at ambient temperature, for 5–8 min to remove the corrosion products.

3. Results and discussion

3.1. Microstructure

Fig. 1 shows microstructures of the transverse and longitudinal facets of Mg–5.23Y, Mg–7.46Y and Mg–13.78Y, after extrusion. Compared with the microstructures of the as-cast alloys, the grains became fine and uniform after extrusion, and the grain sizes of Mg–5.23Y, Mg–7.46Y, and Mg–13.78Y alloys decreased from 1000 μm, 500 μm, and 100 μm to about 50 μm, 40 μm, and 30 μm, respectively [8]. The extrusion line could be clearly seen on the longitudinal facet, whereas the extrusion line along the extrusion direction became clearer with increasing Y content. A large number of small dense equiaxed grains distributed along the extrusion direction. It appears that the microstructures have undergone recrystallization [9]. The parallel shear stripe lines distributed along the extrusion direction on the longitudinal facet, and the parallel shear stripe lines became more visible and denser with increasing of Y content. Large number of fine equiaxed grains distributed on the parallel shear stripe lines. The α-Mg + Mg24Y5 eutectic microstructures is not visible among the grains on the longitudinal facet because that the eutectic microstructures fractured and distributed discretely in the solid solution structure.

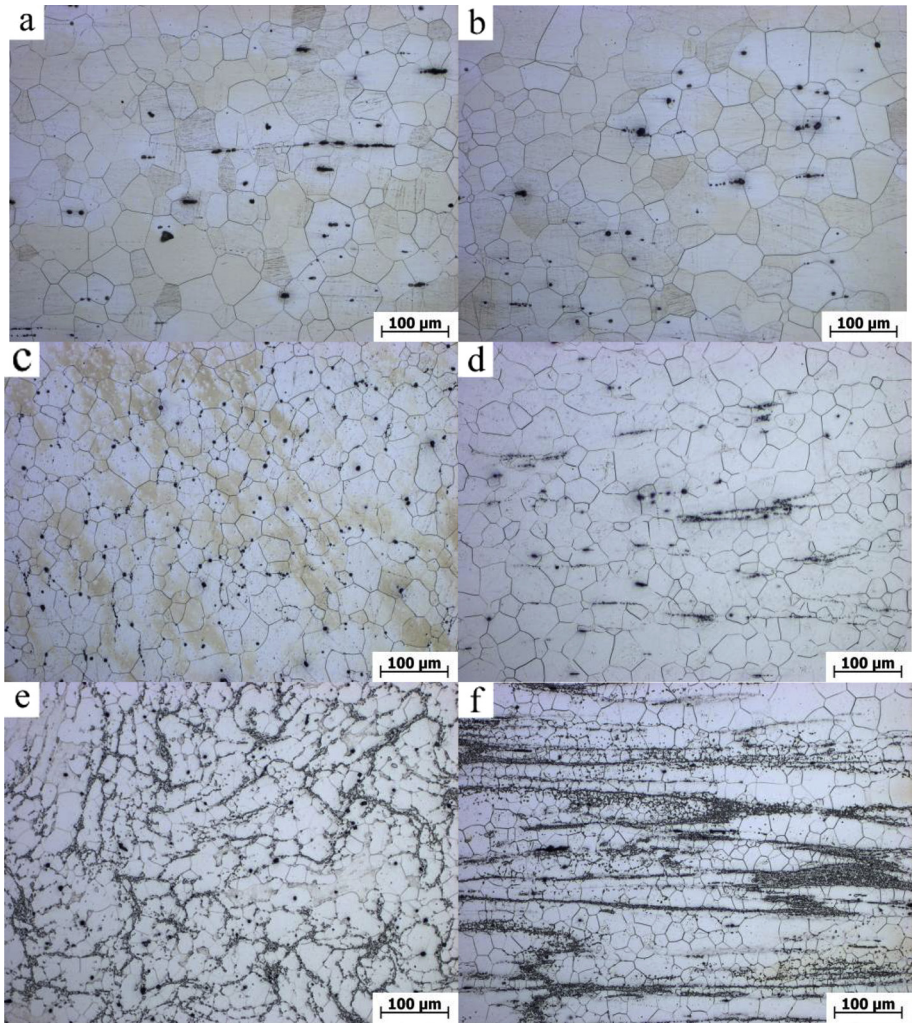

Fig. 1. Microstructure of Mg–Y alloy: Mg–5Y: (a) transversal, (b) longitudinal; Mg–8Y: (c) transversal, (d) longitudinal; Mg–14Y: (e) transversal, (f) longitudinal.

3.2. Corrosion macro-morphologies

Fig. 2 shows macro-morphologies of as extruded samples after 2 h, 4 h, 6 h, 8 h immersion in 3.5 wt.% NaCl solution. Some bubbles appeared on each sample during the soaking time and the bubbles increased quickly with the extension of soaking time, and the corrosion pits appeared on the surface. It could be seen that there were the obvious corrosion pits and insoluble corrosion products attached to the surface when the soaking time was up to 2 h. Both area and depth of the local corrosion increased significantly with the increase of the soaking time. The corrosion area accounted for the great proportion of surface, for 8 h soaking time. From the magnitude of the corroded zone (the black area shown in Fig. 2), it is clear that corrosion resistance of extruded Mg−Y alloy became weaker and weaker by increasing contents of Y. There exist macroscopic preferential corrosion areas on the corroded surface, i.e. some edges are corroded severely than the center and other edges. Plenty of corrosion products are stacked on the corroded surface of the extruded samples; therefore cover some large and deep corrosion pits. Comparing transverse with longitudinal facet after corrosion, it could be found that the local corrosion of longitudinal facet of Mg−5.23Y, Mg−7.46Y and Mg−13.78Y alloys after extrusion was slightly weaker than that of the transverse facet.

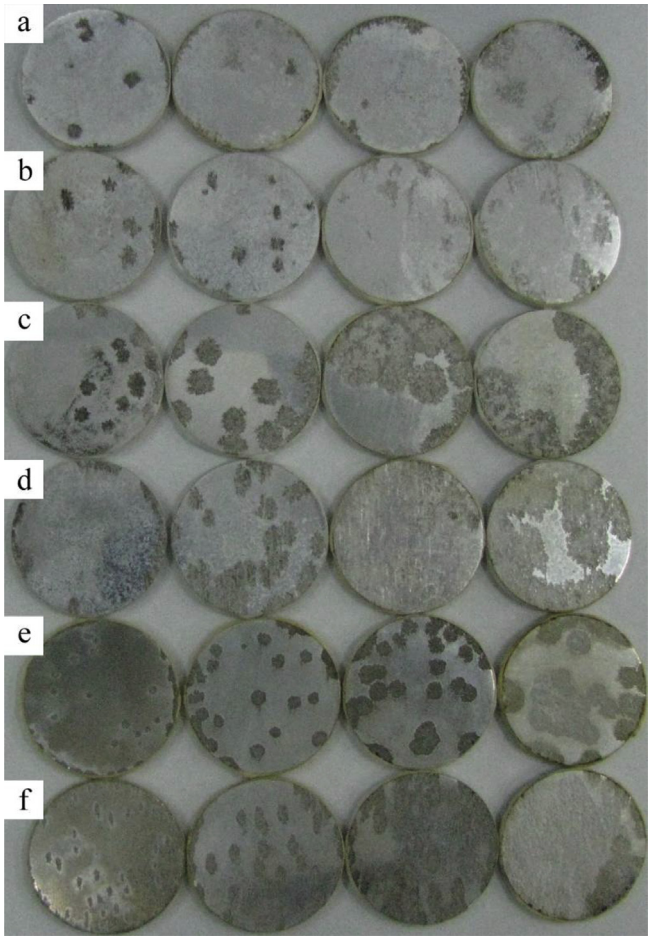

Fig. 2. Macro-morphologies of Mg−Y alloys: Mg−5Y: (a) transversal, (b) longitudinal; Mg−8Y: (c) transversal, (d) longitudinal; Mg−14Y: (e) transversal, (f) longitudinal.

3.3. Weight loss

The most accurate and precise method for the determination of corrosion rates, is the weight loss test [10]. Corrosion rates for samples obtained from weight loss tests are shown in Fig. 3. It can be seen that the corrosion rate of Mg−Y samples increases significantly with the increase of immersion time. The difference of weight loss between Mg−5.23Y and Mg−7.46Y samples is very little, but the corrosion rate of Mg−13.78Y sample is more obviously than that of Mg−5.23Y and Mg−7.46Y samples. The corrosion rate of Mg−Y samples is also increased obviously with increase of Y element, but the corrosion rate of the longitudinal and transversal facets have no significant difference.

3.4. Electrochemical tests

All samples were immersed in 3.5 wt.% NaCl solution for certain time before polarization tests to achieve their stable OCP values. Corrosion potentials (E_{corr}) and corrosion current (I_{corr}) of samples are illustrated in Fig. 4 and Table 1. It shows that the polarization behavior of the extruded alloy has the same changing trend, regardless of the anodic or cathodic part, and shows no self-passivation characteristics. It is clear that these samples have similar polarization curve shapes. The I_{corr} values are determined by extrapolating the linear Tafel segments of the anode and cathode polarization curves. It is obvious that the corrosion potential of samples became nobler with increasing addition of Y element. Further addition of Y element is correlated with the nobler corrosion potentials and the higher corrosion currents. In fact, the corrosion potential value represents a thermodynamic characteristics of a given metal−electrolyte system, but not the kinetics of material corrosion [11]. The I_{corr} values reflect corrosion rate more

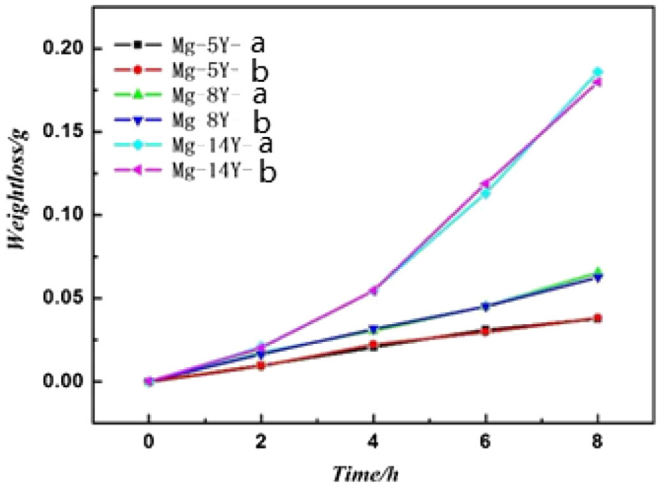

Fig. 3. Curves of weight loss versus immersion time: (a) transversal; (b) longitudinal.

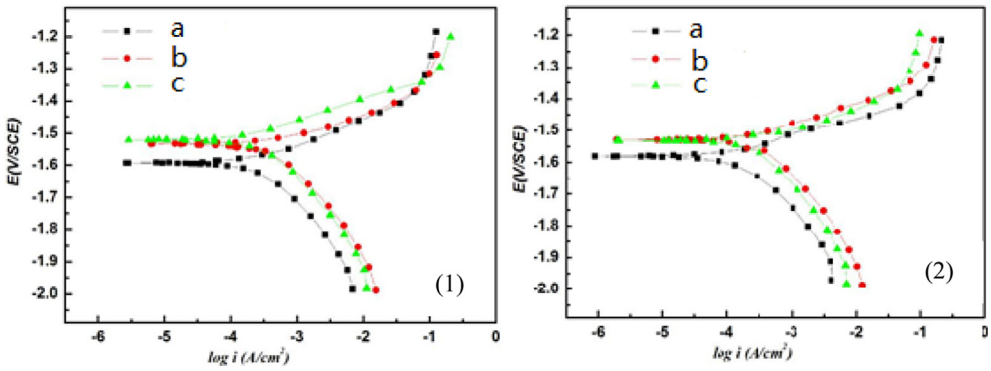

Fig. 4. Polarization curves of Mg–5Y, Mg–8Y and Mg–14Y: (1) transversal; (2) longitude; (a) Mg–5.23Y; (b) Mg–7.46Y; (c) Mg–13.78Y.

accurately than that of E_{corr}. Therefore, the increased I_{corr} values of Mg–5.23Y, Mg–7.46Y, and Mg–13.78Y samples after extrusion correspond to the significantly higher anodic kinetics and lower cathode kinetics. The I_{corr} values increase with increasing Y element, regardless of the longitudinal or transversal facet. However, though the I_{corr} values can reflect the corrosion rate more accurately that of the E_{corr} values, the I_{corr} values only reflect the corrosion rate of the initial immersion time. With the stacked corrosion products and solution of $Mg(OH)_2$, the I_{corr} values do not reflect the true corrosion rate, therefore the direct and accurate reflection of the corrosion rate is the weight loss or the hydrogen evolution

Table 1
E_{corr} and I_{corr} of Mg–5Y, Mg–8Y and Mg–14Y: (a) transversal; (b) longitudinal.

	Mg–5Y		Mg–8Y		Mg–14Y	
	(a)	(b)	(a)	(b)	(a)	(b)
E_{corr} (V)	−1.584	−1.571	−1.532	−1.504	−1.515	−1.531
Log (i)	−3.611	−3.799	−3.453	−3.609	−3.406	−3.607
I_{corr} (10^{-4})	2.449	1.589	3.524	2.460	3.924	2.472

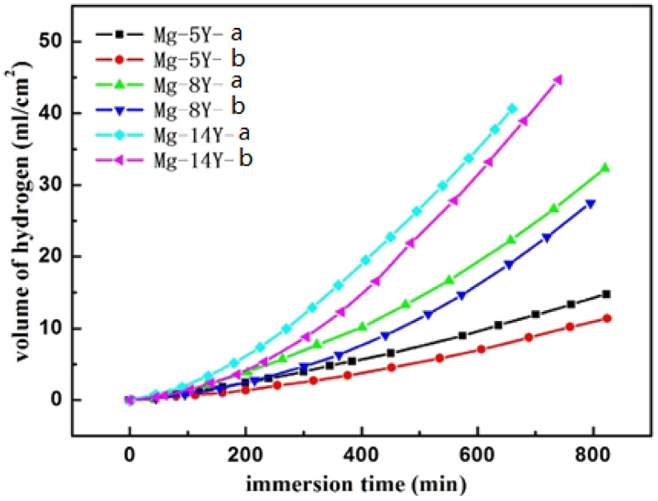

Fig. 5. Curves of hydrogen evolution versus immersion time: (a) transversal; (b) longitudinal.

[12]. These observations indicate that extrusion and addition of Y element have great influence on polarization behaviors of Mg–Y samples, and the trend of increasing corrosion resistance of the three specimens during initial immersion time corresponds to: Mg–13.78Y > Mg–7.46Y > Mg–5.23Y, and the trend of increasing corrosion resistance of the different facet can also be seen as: longitude > transversal.

3.5. Hydrogen evolution

Fig. 5 shows the relationship between hydrogen evolution and immersion time, during the immersion testing samples. From the diagram of hydrogen evolution, three obvious trends can be concluded. Firstly, the corrosion rate increases in aqueous NaCl solution with increasing addition of Y element, and the corrosion rate of Mg–13.78Y sample becomes more than four times higher than Mg–5.23Y during immersion after the 400 min. Secondly, the corrosion rates of all the samples increased firstly obviously then tended to decreased gradually with increasing immersion time. Since the stacked corrosion products have no protective effect on the surface, and the corroded areas increase with time. However, at certain corrosion time, the increase of pH value of the solution is caused by the dissolution of $Mg(OH)_2$ and the stacked corrosion products decrease the corrosion rate [13]. Thirdly, the corrosion rate of transversal facet is worse than that of the longitudinal facet.

4. Conclusions

The grains become finer and uniformed with increasing addition of Y element after extrusion, and the extrusion line can be seen obviously in the longitude facet. The corrosion resistance of Mg–Y alloy after extrusion deteriorates with the addition of Y element, and corrosion rates are decreased in the following order: Mg–13.78Y > Mg–7.46Y > Mg–5.23Y. The corrosion rate of the transversal facet is nobler than that of longitude section during the initial immersion time, as indicated by the polarization curves. However, the transversal facet becomes worse than the longitude section with increasing immersion time. The corrosion rate increases with extension in immersion time, then the corrosion rate tends to

become smooth during the last stage, due to the stacked corrosion products and $Mg(OH)_2$ solution.

Acknowledgment

The authors wished to acknowledge the financial support of the National Key Technology R&D Program of China (nos. 2011BAE22B01 and 2011BAE22B06).

References

[1] K.U. Kainer, P. Bala Srinivasan, C. Blawert, W. Dietzel, Shreir's Corrosion 3 (2009) 2011−2041.
[2] A.J. Davenport, C. Padovani, B.J. Connolly, N.P.C. Stevens, T.A.W. Beale, A. Groso, M. Stampanoni, Electrochemical and Solid-State Letters 10 (2007) C5−C8.
[3] Xin Zhang, Kui Zhang, Xinggang Li, Cong Wang, Hongwei Li, Changshun Wang, Xia Deng, Progress in Natural Science: Materials International 21 (2011) 314−321.
[4] G. Ben-Hamu, D. Eliezer, L. Wagner, Journal of Alloys and Compounds 468 (2009) 222−229.
[5] Vladimir V. Stolyarov, Yuantian T. Zhu, Terry C. Lowe, Ruslan Z. Valiev, Materials Science and Engineering A 303 (2001) 82−89.
[6] W.M. Gan, M.Y. Zheng, H. Chang, X.J. Wang, Journal of Alloys and Compounds 470 (2009) 256−262.
[7] T. Abuleil, N. Hort, W. Dietzel, C. Blawert, Y. Huang, K. Kainer, K. Rao, Transaction of Nonferrous Metals Society of China 19 (2009) 40−44.
[8] Xin Zhang, Kui Zhang, Xia Deng, Hongwei Li, Yongjun Li, Minglong Ma, Ning Li, Yanlong Wang, Progress in Natural Science: Materials International 22 (2012) 169−174.
[9] Hong Yan, Rongshi Chen, Nan Zheng, Jun Luo, Shigeharu Kamado, Enhou Han, Journal of Magnesium and Alloys 1 (2013) 23−30.
[10] E. Poorqasemi, O. Abootalebi, M. Peikari, F. Haqdar, Corrosion Science 51 (2009) 1043−1054.
[11] Dan Song, AiBin Ma, Jinghua Jiang, Pinghua Lin, Donghui Yang, Junfeng Fan, Corrosion Science 52 (2010) 481−490.
[12] S. Mathieu, C. Rapin, J. Hazan, P. Steinmetz, Corrosion Science 44 (2002) 2737−2756.
[13] G.L. Song, A.L. Bowles, David H. Stjohn, Materials Science and Engineering A 366 (2004) 74−86.